Int. J. Heat Mass Transfer. Vol. 33, No 12, pp. 2671–2681, 1990
Printed in Great Britain

0017–9310 90 53.00 + 0.00

Application of the imaginary planes method to three-dimensional systems

A. CHARETTE,† A. LAROUCHE‡ and Y. S. KOCAEFE†

†Groupe de Recherche en Ingénierie des Procédés et Systèmes, Département des Sciences Appliquées, Université du Québec à Chicoutimi, 555, boul. de l'Université, Chicoutimi (Québec), Canada G7H 2B1

‡Alcan International Ltd, 1955, boul. Mellon, P.O. Box 1250, Jonquière (Québec), Canada G7S 4K8

(*Received* 5 *July* 1989 *and in final form* 26 *January* 1990)

Abstract—Three-dimensional (3-D) mathematical formulation of the imaginary planes method (IPM) for the calculation of radiative transfer in rectangular furnaces is presented. In this method, radiative transfer is modelled in terms of chain interaction from zone to zone as opposed to direct interaction in the classical zone method. A number of tests are carried out for gray and real gases as well as different enclosure geometries. The results compare well with those of the zone method. Moreover, considerable reduction in computer time (reduction factor up to 24) has been obtained with respect to the zone method. This feature will allow the IPM to be more easily incorporated into an overall simulation involving the equations of motion, combustion kinetics and transfer of heat and mass.

1. INTRODUCTION

COMMERCIAL numerical codes (e.g. Phoenics, Fluent, Flotran, ...) are becoming more and more popular among the industrial research divisions. These available numerical tools are now used by researchers as the basis of large mathematical models which are made increasingly sophisticated in order to reflect the actual phenomena as closely as possible. However, the complexities of most industrial processes, together with long computation time requirement, still preclude a rigorous simulation of the phenomena involved. Affordable solutions are obtained only through simplified methods.

This paper proposes a simplified method in radiation heat transfer which is the most important heat transfer mode in industrial furnaces. Radiative transfer has been extensively studied over the past three decades. The zone method [1] is known to be the most rigorous of all the 3-D numerical procedures. However, its implementation as part of an overall complex transient model is prohibitive owing to its considerable requirements in computation time. Nevertheless, it is worth mentioning that the accuracy of this technique has led recently some researchers to use it in conjunction with the solution of the Navier–Stokes equations for steady state cases [2, 3]. The Monte Carlo method also gives an 'exact' solution, but its computation requirements are even higher than those of the zone method, and nowadays it is practically confined to a role of reference to which approximate methods are compared to test their validity. Another exact 3-D method is reported by Selçuk [4]. Her proposed method yields a rigorous solution for a box-shaped furnace enclosing a gray gas of uniform absorption coefficient subjected to non-uniform radiative energy source distribution. The results are intended to serve as standards for testing the accuracy of the predictions of approximate radiation models in isolation from the models of flow and combustion. The study is however restricted to black wall enclosures which limits the applicability of the method. The so-called flux methods (see for example ref. [5]), based on an assigned intensity variation over discrete subdivisions of the 4π sr solid angle, lead to a set of differential equations that integrate well with other finite-difference schemes such as those used in solving the Navier–Stokes equations. However, these methods are often over-simplified, especially for cases where the gases are clear and when the heat sink temperatures are low [2]. Lockwood and Shah [6] developed the discrete transfer method which is a combination of Monte Carlo, flux and zone methods. Some applications of this method to industrial processes have been reported in the literature [7, 8]. Recently the method has been adapted to the wide band model for representing non-gray effects [9]. It requires an iterative procedure unless the walls are black. It assumes heat fluxes at the walls, solves the basic transfer equation for radiation beams emitted in predetermined directions and updates the heat fluxes until the convergence is obtained. The iterative nature of this method may result in large computation times for certain applications. Fiveland [10] has adapted the discrete ordinate method (used extensively for solving the neutron transport equation) to the 3-D absorption and scattering of thermal radiative energy. The reported results compare well with those obtained by the zone method for an extinction coefficient of 1.0 m^{-1}. However, since the basic principle of the method is similar to that of the flux methods (solving the radiative transfer equation for a set of discrete direc-

NOMENCLATURE

A surface area [m^2]
a_n, a'_n weighting factor for the nth gray gas when radiation is emitted from a volume or a surface zone, respectively
B_{kj} term containing the reception factors (equation (6))
BM matrix formed from equations (7)–(9)
C_p heat capacity at constant pressure [J kg^{-1} K^{-1}]
CM vector formed from the right-hand side of equations (7)–(9)
D_j term containing the emissive powers and the net heat flows (equation (6))
E black emissive power, σT^4 [W m^{-2}]
f_{jk} reception factor between surface j and surface k
$\overline{gs}_k$ direct interchange area between a volume zone and an enclosing surface k
h convective heat transfer coefficient [W m^{-2} K^{-1}]
I, J, K identification of the subdivisions along the x, y and z coordinates, respectively
K gray gas absorption coefficient [m^{-1}]
L total number of volume zones along the x-axis
M total number of volume zones along the y-axis
$\dot{m}$ mass flow rate [kg s^{-1}]
N total number of gray gases, or total number of volume zones along the z-axis
Q net heat crossing an imaginary plane; subscripts x, y and z for corresponding coordinates [W]
Q_c heat generated by combustion [W]
q heat flux at an imaginary or real surface; q_{k_i} for incident flux on surface k, q_{k_o} for leaving flux, q_k for net flux [W m^{-2}]
T temperature [K]
U overall heat transfer coefficient [W m^{-2} K^{-1}].

Greek symbols
ε emissivity
σ Stefan–Boltzmann constant, 5.67×10^{-8} W m^{-2} K^{-4}.

Subscripts
a ambient
g gas
i incident
i (or j, k) identification of a zone (volume or surface)
n nth gray gas
o leaving
r reference
1, 2, ..., 6 identification of the surfaces enclosing a volume zone (see Fig. 1).

Superscripts
C central volume zone
E east
H high
i neighbouring volume zone
L low
N north
n nth gray gas
S south
SW south-west (other combinations of H, L, E, W, N, S also possible)
W west.

tions within the 4π solid angle), it is not clear if the results would still be as reliable at lower extinction coefficients. The imaginary planes method [11–13] is essentially a simplified zone method. No assumption is made concerning the variation of intensity over the solid angle. The exchange between a given gas zone and its immediate boundaries is calculated as in the zone method, however direct interaction with surrounding gas zones is prohibited. The method was originally developed for one-dimensional systems [11] and then extended to two-dimensional cases [13]. It combines good accuracy and considerably reduced computation time compared to the zone method. Since it requires an integral analysis for the calculation of radiation as opposed to the differential formulation used in the flux methods, the IPM is not directly compatible with the solution of the equations of motion and transfer of heat and mass. Nevertheless, due to its low computation time, it has been used successfully for the modeling of a melter-holder furnace [14] by adopting separate grids for solving radiation and motion/combustion with a proper interface. Although the use of IPM implies added difficulties for its incorporation into the general solution framework, the benefits obtained in terms of accuracy and applicability to different types of furnaces outweigh such problems. This paper briefly describes the general formulation of the 3-D method in rectangular coordinates and presents a number of assessments for typical industrial furnaces.

2. FUNDAMENTALS OF THE IMAGINARY PLANES METHOD (IPM)

The IPM uses the same subdivision principle as that of the zone method, however the interaction between

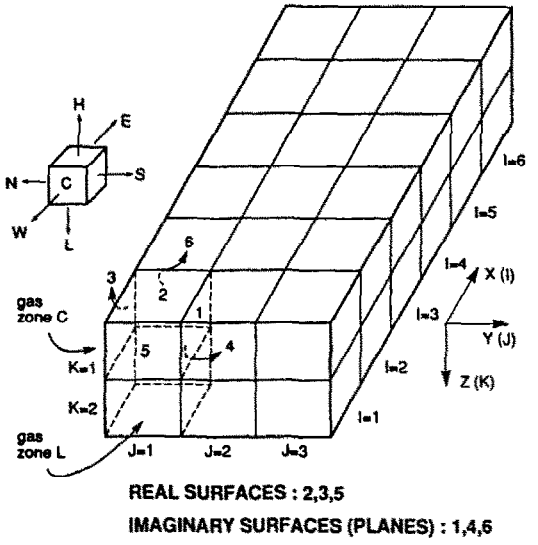

FIG. 1. Identification of the boundaries (by numbers) and of the immediate neighbours (by letters) of a given volume zone C.

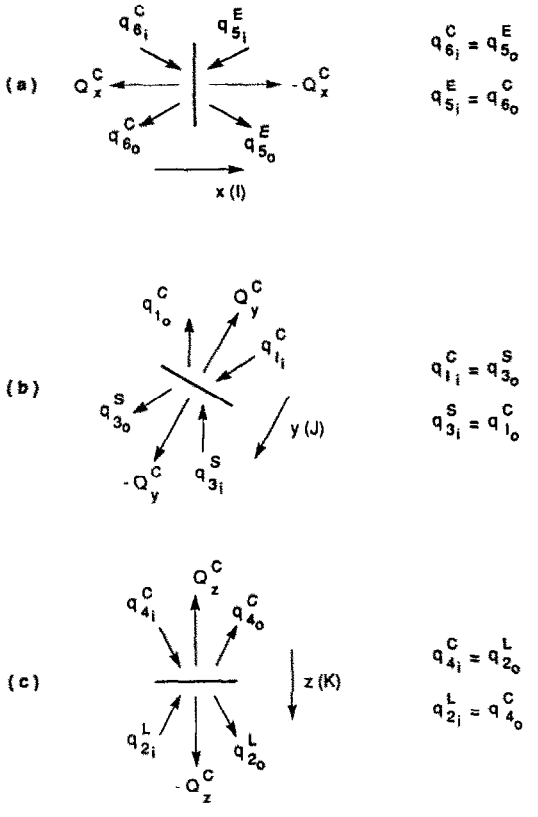

FIG. 2. The coupling principle of the IPM.

zones is more restricted. Two types of surfaces are considered: surfaces on the enclosure walls referred to as real surfaces (not in the sense of radiatively selective surfaces) and imaginary planes separating the adjacent volume zones. Figure 1 depicts these surfaces and explains the identification of the boundaries (by numbers) and of the immediate neighbours (by letters) of a given volume zone C. According to the IPM, each volume zone has a direct view only of its own boundaries. However, the adjacent volume zones are linked through radiative heat fluxes crossing the imaginary planes, providing an indirect interaction between all the zones as opposed to the direct interaction in the zone method. Figure 2 describes the linking procedure between the zones through the imaginary planes in three directions. The subscripts i and o stand for 'incident' and 'leaving', respectively. Q is the net heat flow rate, and it will be defined by equation (3). The linking principle between adjacent volume zones is that the incident flux on an imaginary plane coming from a given volume is equal to the leaving flux from the same plane directed towards the adjacent volume (that is the flux is continuous through the imaginary plane, e.g. $q^{C}_{6_i} = q^{E}_{5_o}$). The IPM allows the radiative transfer in each volume zone to be expressed in terms of heat fluxes or temperatures of its six faces, which offers the considerable advantage that the interchange areas can now be calculated zone by zone independently. The linking procedure then takes care of the interdependence between zones in the enclosure. An abridged mathematical formulation is given below. Emphasis is put on the extension of the method to 3-D systems. Detailed derivations of the equations may be found in the previously published work on this topic [11, 13, 17].

Irradiation $q^{C}_{k_i}$ of surface k of a given volume zone C is due to radiative heat received from gas C and from the six faces (real and imaginary) by which zone C is bounded

$$A^{C}_{k} q^{C}_{k_i} = \sum_{j=1}^{6} A^{C}_{j} f^{C}_{jk} q^{C}_{j_o} + \overline{gs}^{C}_{k} E^{C}_{g} \tag{1}$$

where f_{jk} is the reception factor between surface j and surface k according to the terminology first introduced by Hottel and Cohen [1], and $\overline{gs}_k$ is the direct interchange area between the gas and surface k. If the surface is real, the above equation combined with a heat balance leads to

$$q^{C}_{k_o} - (1-\varepsilon^{C}_{k}) \sum_{j=1}^{6} f^{C}_{kj} q^{C}_{j_o} = \varepsilon^{C}_{k} E^{C}_{k} + (1-\varepsilon^{C}_{k}) \frac{E^{C}_{g} \overline{gs}^{C}_{k}}{A^{C}_{k}}. \tag{2}$$

On the other hand, a heat balance performed on an imaginary surface (plane) gives the general equation (see Fig. 2)

$$Q^{C}_{k} = (q^{C}_{k_o} - q^{C}_{k_i}) A^{C}_{k} \tag{3}$$

where, by convention, the net heat flow rate Q^{C}_{k} is taken as positive in the inward direction within zone C and opposite to the coordinate directions. Replacing the incident fluxes $q^{C}_{k_i}$ in equation (3) with the leaving fluxes in the adjacent volume zones based on the linking procedure and rearranging leads to the following relations:

$$\frac{Q_x^C}{A_x^C} = q_{6_o}^C - q_{5_o}^E; \quad \frac{Q_y^C}{A_y^C} = q_{1_o}^C - q_{3_o}^S;$$

$$\frac{Q_z^C}{A_z^C} = q_{4_o}^C - q_{2_o}^L. \tag{4}$$

Incorporation of equation (1) in equation (3) yields

$$q_{k_o}^C - \sum_{j=1}^{6} f_{kj} q_{j_o}^C = \frac{Q_k^C}{A_k^C} + \frac{E_g^C \overline{gs}_k^C}{A_k^C}. \tag{5}$$

Equations (2) and (5) apply for real surfaces and imaginary planes, respectively, and their similarity can be exploited to produce a single relation valid for both cases [13]

$$q_{k_o}^C = \sum_{j=1}^{6} B_{kj}^C D_j^C, \quad k = 1, 2, \ldots, 6 \tag{6}$$

where B_{kj}^C is expressed in terms of the reception factors between surfaces, while D_j^C contains the emissive powers of the gas and surface zones as well as the net heat flows at the imaginary planes. Introducing equation (6) in equation (4) and rearranging terms results in the following three equations:

for the x-coordinate

$$\frac{1}{A_x}[Q_x^W B_{65}^C + Q_x^C(1 - B_{66}^C - B_{55}^E) + Q_x^E B_{56}^E]$$

$$+ \frac{1}{A_y}[Q_y^N B_{63}^C - Q_y^C B_{61}^C - Q_y^{NE} B_{53}^E + Q_y^E B_{51}^E]$$

$$+ \frac{1}{A_z}[Q_z^H B_{62}^C - Q_z^C B_{64}^C - Q_z^{HE} B_{52}^E + Q_z^E B_{54}^E]$$

$$= \sum_{j=1}^{6} B_{6j}^C \left(\varepsilon_j^C E_j^C + \frac{(1-\varepsilon_j^C) E_g^C \overline{gs}_j^C}{A_j^C}\right)$$

$$- \sum_{j=1}^{6} B_{5j}^E \left(\varepsilon_j^E E_j^E + \frac{(1-\varepsilon_j^E) E_g^E \overline{gs}_j^E}{A_j^E}\right); \tag{7}$$

for the y-coordinate

$$\frac{1}{A_x}[Q_x^W B_{15}^C - Q_x^C B_{16}^C - Q_x^{SW} B_{35}^S + Q_x^S B_{36}^S]$$

$$+ \frac{1}{A_y}[Q_y^N B_{13}^C + Q_y^C(1 - B_{11}^C - B_{33}^S) + Q_y^S B_{31}^S]$$

$$+ \frac{1}{A_z}[Q_z^H B_{12}^C - Q_z^C B_{14}^C - Q_z^{HS} B_{32}^S + Q_z^S B_{34}^S]$$

$$= \sum_{j=1}^{6} B_{1j}^C \left(\varepsilon_j^C E_j^C + \frac{(1-\varepsilon_j^C) E_g^C \overline{gs}_j^C}{A_j^C}\right)$$

$$- \sum_{j=1}^{6} B_{3j}^S \left(\varepsilon_j^S E_j^S + \frac{(1-\varepsilon_j^S) E_g^S \overline{gs}_j^S}{A_j^S}\right); \tag{8}$$

for the z-coordinate

$$\frac{1}{A_x}[Q_x^W B_{45}^C - Q_x^C B_{46}^C - Q_x^{LW} B_{25}^L + Q_x^L B_{26}^L]$$

$$+ \frac{1}{A_y}[Q_y^N B_{43}^C - Q_y^C B_{41}^C - Q_y^{LN} B_{23}^L + Q_y^L B_{21}^L]$$

$$+ \frac{1}{A_z}[Q_z^H B_{42}^C + Q_z^C(1 - B_{44}^C - B_{22}^L) + Q_z^L B_{24}^L]$$

$$= \sum_{j=1}^{6} B_{4j}^C \left(\varepsilon_j^C E_j^C + \frac{(1-\varepsilon_j^C) E_g^C \overline{gs}_j^C}{A_j^C}\right)$$

$$- \sum_{j=1}^{6} B_{2j}^L \left(\varepsilon_j^L E_j^L + \frac{(1-\varepsilon_j^L) E_g^L \overline{gs}_j^L}{A_j^L}\right). \tag{9}$$

The above expressions are written in a general form to facilitate the computer programming. For the case of volume zone C illustrated in Fig. 1, the following terms are set equal to zero: Q_x^W, Q_x^N, Q_x^S, Q_x^{SW}, Q_x^{LW}, Q_y^{NE}, Q_y^{LN}, Q_z^{HE}, Q_z^{HS}, Q_z^H, ε_1^C, ε_4^C, ε_6^C, ε_1^E, ε_4^E, ε_5^E, ε_6^E, ε_1^S, ε_3^S, ε_4^S, ε_6^S, ε_1^L, ε_2^L, ε_4^L, ε_6^L. These equations are applied to each corresponding imaginary plane generated by the grid used for the furnace. Let L, M and N be the number of volume zones (divisions) in directions x, y and z, respectively. Then, the total number of imaginary planes (equal to the total number of unknown Q's in the corresponding equations) is equal to: $(L-1)MN + (M-1)LN + (N-1)LM$. A sparse banded matrix system of the same dimension is thus obtained, and it can be condensed to

$$[BM]\{Q\} = \{CM\} \tag{10}$$

where matrix $[BM]$ contains the interchange areas and vector $\{CM\}$ contains the emissive powers of the gas and real surface zones. This linear equation system is best solved by a $L\backslash U$ technique. Furthermore, if some (or all) of the volume and surface temperatures are unknown (as it is usually the case), then heat balances have to be written for each zone of unknown temperature.

For a gas zone

$$Q_c^C + \sum_{\substack{k \\ \text{(real surfaces)}}} [A_k^C q_k^C + h^C A_k^C (T_k^C - T_g^C)]$$

$$+ \sum_{i=1}^{6} \dot{m}^i C_p^i (T_g^i - T_r) - \dot{m}^C C_p^C (T_g^C - T_r)$$

$$+ (Q_x^C - Q_x^W) + (Q_y^C - Q_y^N) + (Q_z^C - Q_z^H) = 0 \tag{11}$$

where Q_c^C is the heat released due to combustion in zone C, h^C the heat transfer coefficient between the surface zone (with temperature T_k^C) and the adjacent volume zone (with temperature T_g^C), $\dot{m}^i$ is the mass flow rate entering volume C from surrounding volume zones (with heat capacity C_p^i and temperature T_g^i).

For a real surface zone

$$A_k^C q_k^C + h^C A_k^C (T_k^C - T_g^C) + U A_k^C (T_k^C - T_a) = 0 \tag{12}$$

where U is the overall heat transfer coefficient between inner wall temperature T_k^C and ambient temperature T_a.

It is seen from the above expressions that allowance is made for combustion, convection and arbitrary flow pattern (the latter through the term

$$\sum_{i=1}^{6} \dot{m}^i C_p^i (T_g^i - T_t)$$

of equation (11)). The distribution of the combustion and flow patterns can be either prescribed or calculated by solving the combustion kinetics and Navier–Stokes equations. Since the purpose of this work is to assess the IPM, these will be prescribed here. The solution of the problem is then obtained by an iterative procedure as follows: (1) an initial temperature field is assumed; (2) the Q's are computed by equation (10); (3) the q_{k_o}'s are found by equation (6); (4) the net fluxes at the walls are obtained by $q_k^C = (E_k^C - q_{k_o}^C)\varepsilon_k^C/(1-\varepsilon_k^C)$; (5) the new temperature distribution is obtained by solving the non-linear equations (11) and (12) using the Newton–Raphson technique; (6) these temperatures are compared with the previous ones, and if the difference is less than a given tolerance, the solution has converged; if not, the procedure is repeated starting from step 2 until the convergence is obtained.

2.1. *Extension to real gases*

To adapt the formulation to a real gas medium, Hottel's well-known weighted sum of gray gases formulation is used [15]. The chosen technique is similar to that used in the zone method, except that the weighting coefficients are assigned to the direct interchange areas rather than the total interchange areas. For example, in the presence of a real gas, equation (1) is rewritten as

$$A_k^C q_{k_i}^C = \sum_{j=1}^{6} \left[\sum_{n=1}^{N} a_n'(T_j^C, T_g^C) A_j^C f_{jk}^{n,C} \right] q_{j_o}^C + \sum_{n=1}^{N-1} a_n(T_g^C) \bar{g}s_k^{n,C} E_g^C \quad (13)$$

where a_n' and a_n are the weighting coefficients for the absorptivity and the emissivity of the gas. The rest of the mathematical formulation is modified accordingly. However, two difficulties arise. First, the B values in equation (6) are now dependent on temperature and so is, as a consequence, the matrix $[BM]$ in equation (10). Therefore, in calculating the Jacobian for the solution of equations (11) and (12), the partial derivative of Q with respect to a given temperature T_i is expressed as

$$\left\{\frac{\partial Q}{\partial T_i}\right\} = [BM]^{-1} \left\{\frac{\partial CM}{\partial T_i}\right\} + \frac{\partial}{\partial T_i}[BM]^{-1}\{CM\} \quad (14)$$

which makes the solution more difficult especially for 3-D cases. Owing to the relatively moderate variation of the weighting factors a and a' with respect to temperature, the recommended procedure is to neglect the last partial differential in equation (14) and to re-evaluate $[BM]$ at each iteration with the updated temperature. The second difficulty is apparent from the examination of equation (13). It is seen that $a_n'(T_j, T_g)$ is to be evaluated on the basis of the temperatures of the six faces enclosing a given volume zone. These faces can be imaginary planes for which T_j is immaterial since radiation passing through them is of many different sources (gas and surface). There is no clear solution to this problem. Different suggestions have been made, among which: taking T_j equal to the geometric mean value of the gas temperatures on both sides of the plane [13], or using the closest solid temperature [17]. However, the authors feel that the full assessment of this point has not yet been made and, therefore, no general rule can be drawn for the moment. Thus, even though results from the IPM were found to compare well with those obtained from the zone method for real gases, at this stage the utilization of IPM offers a safer basis for the case of a gray medium.

3. RESULTS

To assess the IPM method, a series of tests were performed on different types of furnaces.

3.1. *Test 1*

The first geometry chosen is the one illustrated in Fig. 1 which corresponds to a typical elongated combustion chamber of an aluminium melter/holder. This case is fully described in Table 1 and Fig. 3. The liquid metal that constitutes the bottom of the furnace is held constant at 1033 K and all the other surface and gas temperatures are unknown. The total heat release by combustion (natural gas) and the mass flow rate at the burner are respectively 4213 kW and 1.754 kg s^{-1}, corresponding to typical values in the industrial operation. The gas medium is considered as gray with an absorption coefficient of 0.175 m^{-1}. Such a gas is relatively transparent and is therefore a good medium for testing the validity of a simplified method such as the IPM. In principle, the IPM should give better results in dark gases since the formulation is based on partial interaction between zones. The chosen grid is $6 \times 3 \times 4$ (x, y, z), but this can be changed at will since the interchange areas are calculated by a Monte Carlo method which allows high flexibility in the sizing of the grid. The results of the simulation are presented in Fig. 4 for the heat transferred to the liquid metal at $J = 1$ and 2 (part (a)), the temperature of the roof at the same location (part (b)) and the gas temperature averaged over the height of the furnace at $J = 2$ (part (c)). The IPM is compared with the zone method which is taken as the rigorous solution. It is seen that the results are in good agreement. The average computational errors are 4.4, 3.4 and 0.5% for parts (a), (b) and (c), respectively. The computation times on a VAX-785 were 1099 and 74 s for the zone method and the IPM respectively, giving a time ratio of 14.9.

Table 1. Data used in test 1 for the elongated furnace

Model inputs	Remarks and numerical values
PRESCRIBED PATTERNS:	
Combustion	see Fig. 3(a)
Flow field	see Fig. 3(b)
PHYSICAL PARAMETERS:	
Gas absorption coefficient K	0.175 m^{-1}
Direct interchange areas	calculated by Monte Carlo
Refractory emissivity	0.7
Charge (bottom) emissivity	0.6
Nature of gas	gray
Size of the furnace (x, y, z)	$10.75 \times 3.75 \times 1.2$ m
Number of subdivisions (x, y, z)	$6 \times 3 \times 4$
Overall heat transfer coefficient (from inside surface to environment)	
—charging side	1.3 W m^{-2} K^{-1}
—side opposite to the charging doors	0.86 W m^{-2} K^{-1}
—roof	1.37 W m^{-2} K^{-1}
—burner face and opposite face	0.75 W m^{-2} K^{-1}
Convective heat transfer coefficient	
—burner face and opposite face	50 W m^{-2} K^{-1}
—other faces	25 W m^{-2} K^{-1}
Composition of combustion gas (volume basis)	CO_2 8.9, H_2O 17.7, O_2 1.3, N_2 72.1%
Ambient temperature	298 K
Temperature at burner inlet	333 K
Charge temperature	1033 K

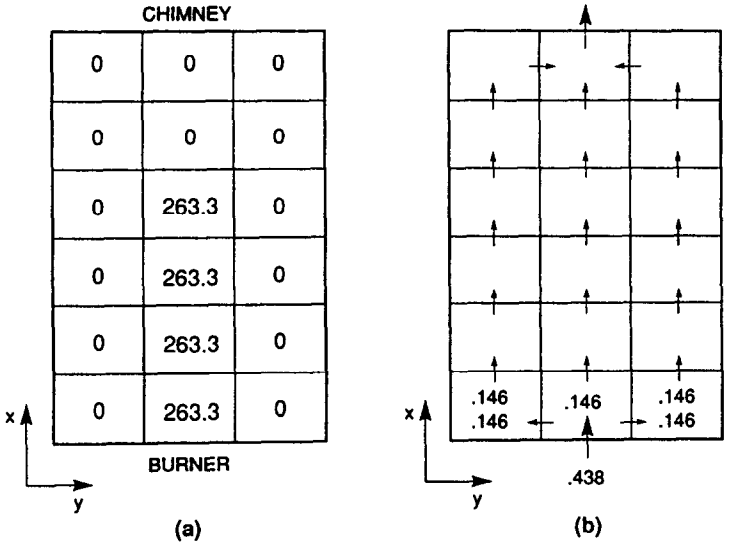

FIG. 3. (a) Prescribed combustion distribution for Test 1 (kW); (b) prescribed flow field (kg s^{-1}). The indicated values are relative to each subdivision along the z-axis (four subdivisions in this case); they must thus be multiplied by 4 to obtain the total values for the furnace.

3.2. *Test 2*

The same example has been worked out based on the real gas behaviour for which the molar ratio H_2O/CO_2 was taken equal to 2, characteristic of the combustion products of natural gas (the full composition is given in Table 1). Results are shown in Fig. 5 for the parallelepiped gas portion $J = K = 2$. As explained previously, the solution is dependent on the immaterial temperatures of the imaginary planes. Three cases have been tested here. In case 1, all the imaginary planes were assigned the temperature of the liquid metal (1033 K); in cases 2 and 3, they were assigned, respectively, the average temperature of all the refractories enclosing the furnace and the average temperature of the real surface zones parallel and opposed on both sides to each imaginary plane. The

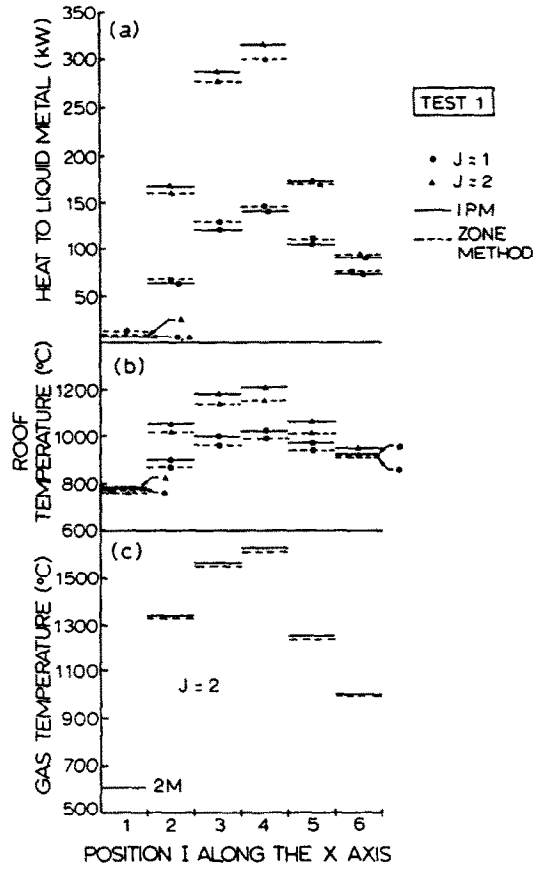

FIG. 4. Results for Test 1 (elongated furnace, gray gas with $K = 0.175\ m^{-1}$): (a) heat to the liquid metal at $J = 1$ and 2; (b) roof temperature at the same locations; (c) gas temperature averaged over the height of the furnace at $J = 2$ (2M means that the two methods give similar results).

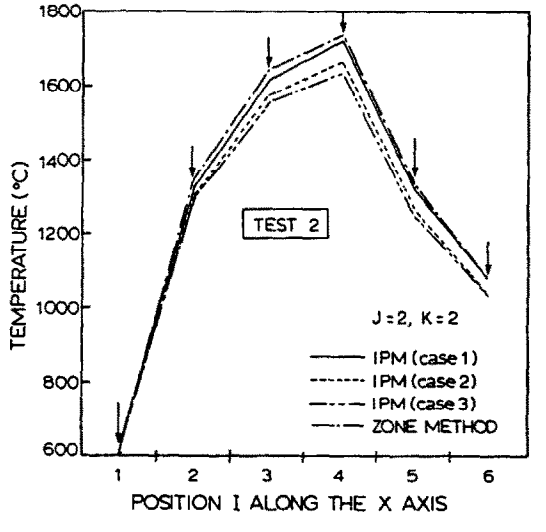

FIG. 5. Results for Test 2 (elongated furnace, real gas). The arrows indicate the locations of the calculated values. Continuous lines between these points have no physical meaning, however they are used here in place of the bar diagram (see Fig. 4) to avoid overloading the figure.

temperature dependent weighting coefficients introduced in equation (13) were calculated according to the procedure suggested by Smith *et al.* [18]. Four gray gases were considered, one being the clear gas with $K = 0\ m^{-1}$. It is apparent from Fig. 5 that the best results are obtained for the first case, i.e. when the bottom surface temperature is used as the imaginary plane temperature in the calculations (average percentage error: 1%). This surface has the lowest temperature of all the surfaces of the enclosure and is by far the most absorbing. Unfortunately, at this stage, it cannot be stated positively that the most absorbing surface should be used in all other systems. Nevertheless, it can be pointed out that case 1 gives better results than when the imaginary planes are assigned mean temperatures of the gas zones on both sides of the planes as reported in ref. [13]. For this case, the computation times were 4744 and 413 s for the zone method and the IPM, respectively (ratio = 11.5).

3.3. *Test 3*

To further test the method, the cross section of the furnace was changed to a square of 5 m × 5 m (still 10.75 m long), and the energy released by combustion and the total flow rate were doubled without changing however the relative distribution of these quantities.

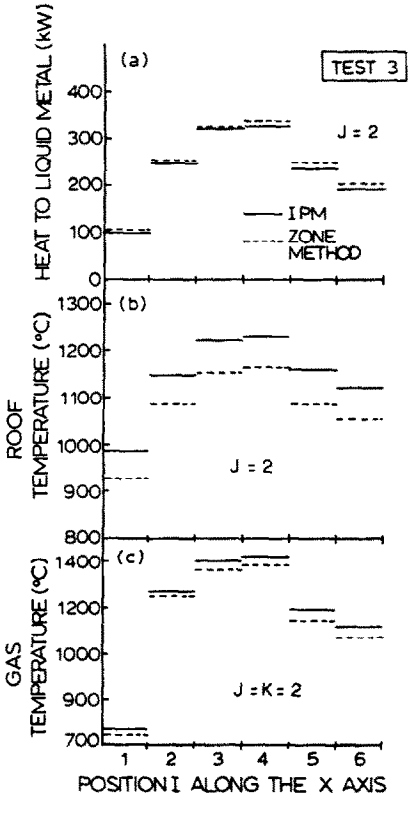

FIG. 6. Results for Test 3 ($5 \times 5 \times 10.75$ m furnace, gray gas with $K = 0.175\ m^{-1}$). Parts (a) and (b) are for $J = 2$ and part (c) for $J = K = 2$.

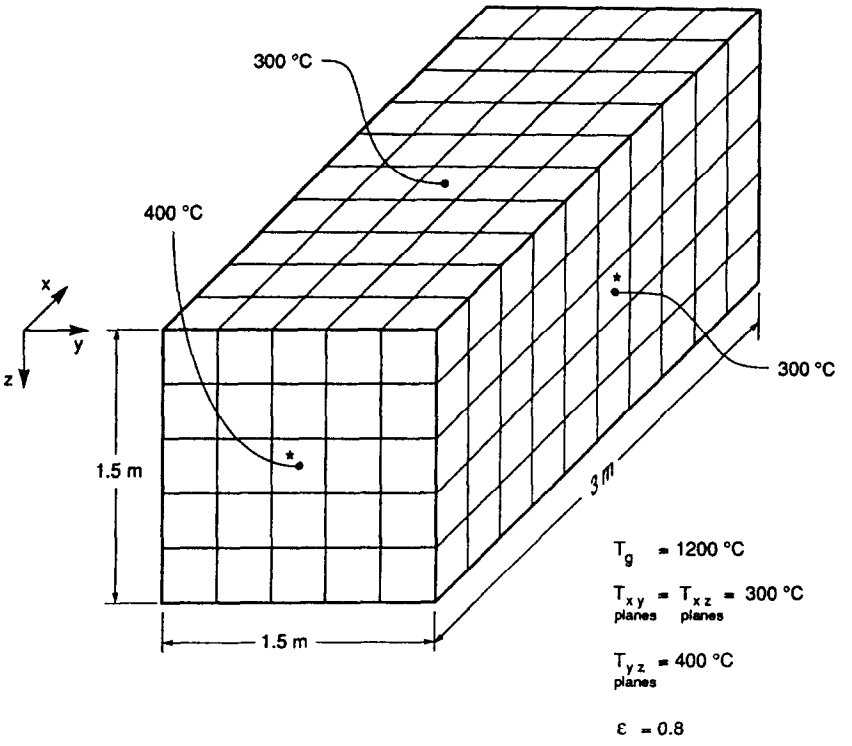

FIG. 7. Description of the enclosure used in Test 4.

The gas was taken as gray. The rest of the characteristics remained unchanged. This modified furnace is a more severe test for the IPM. The furnace is no longer of the elongated type, and the radiative transfer is important in every direction (in the previous case, the axial heat fluxes were small compared to the transversal ones). The results are given in Fig. 6 for the same variables as in Fig. 4. Note however that the gas temperatures are reported for $J = K = 2$ instead of values averaged over the height. It is seen that the discrepancies between the two methods are of the same order as the previous ones: the average errors are 4, 6.1 and 3.5% on the heat to the liquid metal, the roof temperature and the gas temperature, respectively. The computation time ratio between the two methods was the same as in Test 1.

3.4. *Test 4*

The purpose of this last test is to evaluate the influence of the gas absorption coefficient K. The assessment is made for a case of pure radiation, all temperatures of the volume and surface zones being prescribed, which means that the solution of the nonlinear set of equations of the type (11) and (12) is bypassed. Hence, the emphasis is put here on the basic principle of the IPM. Since the interaction between zones is established indirectly, it is logical to question the validity of the method at very low absorption coefficients, in which case the exchange between distant zones also become important. The enclosure chosen is described in Fig. 7. It is a $1.5 \times 1.5 \times 3$ m (x, y, z) box-shaped furnace with gas, lateral wall and end wall temperatures at 1200, 300 and 400°C, respectively. The emissivity of all the surfaces is 0.8. The chosen grid is $10 \times 5 \times 5$ and computation is done for $K = 0.15$ and 0.05 m^{-1}. Because of the symmetry, results may be reported only for the planes marked with an asterisk. By comparing parts (a) and (b) of Fig. 8, it can be seen that the discrepancies between the IPM and the zone method do not increase with decreasing gas absorption coefficient K (identical average error of 8.7% for both $K = 0.15$ and 0.05). The only significant discrepancies ($\sim$25%) are localized at the corners of the y–z plane. For $K = 0.05$, the computation time with the IPM was 267 s compared to 3170 s with the zone method (time ratio = 11.9).

4. COMPUTATION TIME

A comparison of the computation time for both methods is given above. It is worthwhile however to examine more closely its apportionment. In both the IPM and the zone method two different computation times can be identified. The first one is the time for the calculation of the direct interchange areas (dIA) by the Monte Carlo method. For the IPM, the number of dIA's to be evaluated is $42N_D$, where N_D is the number of finite volume zones of distinct size and gas absorption coefficient. N_D is equal to 1 for a case of uniform grid and uniform gas absorption coefficient. In the zone method, the number of dIA's is equal to

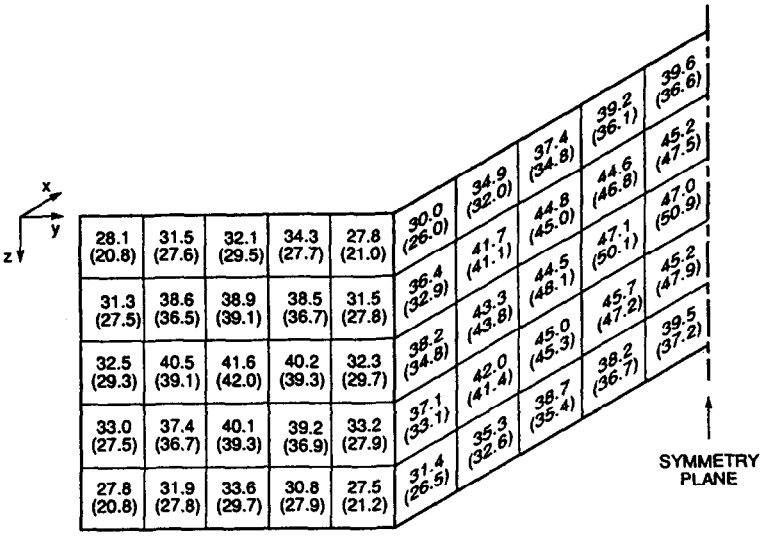

(a) K = 0.15

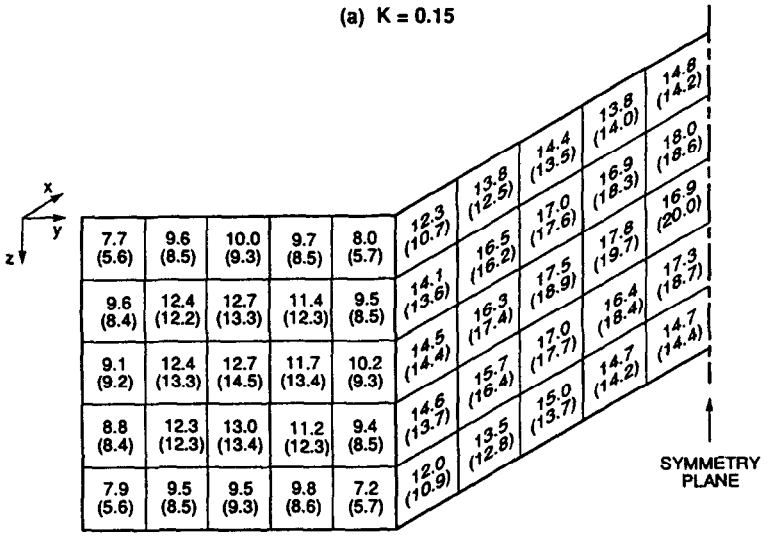

(b) K = 0.05

FIG. 8. Comparison of the IPM and the zone method (Test 4) with $K = 0.15\ m^{-1}$ (part (a)) and $K = 0.05\ m^{-1}$ (part (b)). Results are reported for the net heat fluxes in kW m^{-2}. Values in parentheses are for the IPM.

$42N^2$ where N is the total number of finite volumes in the domain regardless of the sizes of the volume zones and the gas absorption coefficient distribution. Hence, it can be inferred that the IPM reduces computation time considerably, especially for the case of uniform grid/uniform gas absorption coefficient. It must be pointed out however that this comparison is not perfect, since the zone method goes one step further by evaluating the total interchange areas which adds to the computation time (it increases considerably if the emissivities of the real surfaces are low). The second time is related to the calculation of radiative heat fluxes and to the procedure for the convergence of heat balances on the surface and volume zones, the combination of which will be referred to as the *iteration time*. Since both methods use the Newton–Raphson algorithm for solving the heat balances, there is no significant difference in computation time in this regard. However, due to limited interaction of the IPM with the neighbouring zones, time used for obtaining the radiative heat fluxes is much less with this method.

Figure 9 shows how the time ratio (defined as the ratio of the time required with the zone method to that with the IPM) varies with respect to the number of finite volumes on a VAX-785 for the case of a gray gas where all the zone temperatures are unknown. It can be seen from the figure that iteration time is the

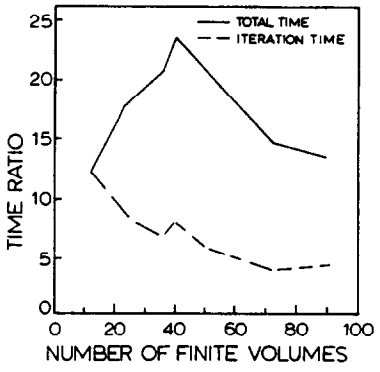

FIG. 9. Effect of the grid size on the time ratio.

limiting factor since the total time ratio would be continuously increasing if it were dependent solely on the interchange area calculation. This limiting phenomenon can be explained as follows. The IPM uses two levels of matrix calculations to solve for radiative fluxes whereas the zone method uses only one. For a fine grid, the matrices are large and, since the computation time varies approximately with the third power of the matrix order, the time saving is somewhat reduced. For commonly used grid sizes (70–90 finite volumes), the total time ratio is about 14, and it can go up to 24 if 40 volume zones are used.

5. CONCLUSION

The 3-D mathematical formulation of the imaginary planes method in rectangular coordinates has been presented. Assessment has been done for a number of cases which demonstrate accuracy of the IPM. Cases treated include elongated and short furnaces, different absorption coefficients, gray and real gases. The interesting feature of the method lies in the fact that each volume zone, while being linked to the adjacent volume zones by the net radiative heat fluxes, is still radiatively autonomous from the point of view of the interchange area calculation. The imaginary planes preclude a direct radiative exchange with the other zones in the enclosure. This characteristic leads to appreciable savings in computation time. Absolute time saving capability becomes very important when transient processes are being studied. Furthermore, some cases which are very difficult to handle by some other methods are solved easily by the IPM such as the geometrical irregularities in the enclosure. It should also be noted that, even if the flow patterns used in the current assessment were simple, more complex patterns can easily be handled [13]. The IPM is presently being incorporated into a general model of an aluminium casting furnace.

Acknowledgement—This work has been made possible by an operating grant of the Natural Sciences and Engineering Research Council of Canada (NSERC).

REFERENCES

1. H. C. Hottel and E. S. Cohen, Radiant heat exchange in a gas-filled enclosure: allowance for non-uniformity of gas temperature, *A.I.Ch.E. Jl* **4**, 3–14 (1958).
2. L. Post, A mathematical model of the combustion chamber in a glass furnace. In *Numerical Methods in Thermal Problems*, Vol. 5, part 1, p. 884. Pineridge Press, Swansea (1987).
3. D. Trivic, Mathematical modelling of three dimensional turbulent flow with combustion and radiation, Ph.D. Thesis, Department of Chemical Engineering, University of New Brunswick, Fredericton, Canada (1987).
4. N. Selçuk, Exact solutions for radiative heat transfer in box-shaped furnaces, *J. Heat Transfer* **107**, 648–655 (1985).
5. A. G. de Marco and F. C. Lockwood, A new flux model for the calculation of radiation in furnaces, *Rir. Combust.* **29**, 184–196 (1975).
6. F. C. Lockwood and N. G. Shah, New radiation solution method for incorporation in general combustion prediction procedures, *The Eighteenth Symp. (Int.) on Combustion*, pp. 1405–1414. The Combustion Institute, Pittsburgh (1981).
7. A. D. Gosman, F. C. Lockwood, I. E. A. Megahed and N. G. Shah, The prediction of the flow, reaction, and heat transfer in the combustion chamber of a glass furnace, *Proc. Eighteenth Aerospace Sciences Meeting*, Paper 80-0016, Pasadena (1980).
8. A. S. Abbas, F. C. Lockwood and A. P. Salooja, The prediction of the combustion and heat transfer performance of a refinery heater, *Combust. Flame* **58**, 91–101 (1984).
9. P. Docherty and M. Fairweather, Predictions of radiative transfer from nonhomogeneous combustion products using the discrete transfer method, *Combust. Flame* **71**, 79–87 (1988).
10. W. A. Fiveland, Three-dimensional radiative heat transfer solutions by the discrete-ordinates method, *The 24th Natn. Heat Transfer Conf. and Exhibition (ASME), Fundamentals and Applications of Radiation Heat Transfer*, HTD-Vol. 72, pp. 9–18 (1987).
11. B. Ström, A simple heat transfer model for furnaces based on the zoning method, *Wärme- und Stoffübertr.* **13**, 47–52 (1980).
12. Z. Kolenda, S. Slupek and J. Szmyd, Application of the imaginary surfaces method for the simulation of the temperature in the combustion process of liquid fuel, *Metalurgia Odlewnictwo* **10**, 135–149 (1984).
13. A. Charette, F. Erchiqui and Y. S. Kocaefe, The imaginary planes method for the calculation of radiative heat transfer in industrial furnaces, *Can. J. Chem. Engng* **67**, 378–384 (1989).
14. A. Charette, R. T. Bui, Y. S. Kocaefe, A. Larouche and G. Simard, Mathematical modelling of an aluminium melting furnace, *Proc. 1989 Spring Tech. Meeting of the Combustion Institute (Canadian Section)*, pp. 97–99 (1989).
15. H. C. Hottel and A. F. Sarofim, *Radiative Transfer*. McGraw-Hill, New York (1967).
16. F. R. Steward and Y. S. Yocaefe, Total emissivity and absorptivity models for carbon dioxide, water vapor and their mixtures, *Proc. Eighth Int. Heat Transfer Conf.*, Vol. 2, pp. 735–740 (1986).
17. A. Larouche, Couplage de la méthode des plans imaginaires en trois dimensions et du logiciel Phoenics pour la modélisation de la chambre de combustion de fours industriels, M.Sc. Thesis, Department of Applied Sciences, University of Quebec at Chicoutimi, Canada (1988).
18. T. F. Smith, Z. F. Shen and J. N. Friedman, Evaluation of coefficients for the weighted sum of gray gases model, *J. Heat Transfer* **104**, 602–608 (1982).

LA METHODE DES PLANS IMAGINAIRES APPLIQUEE A DES SYSTEMES TRIDIMENSIONNELS

Résumé—On présente la formulation mathématique de la méthode des plans imaginaires pour le calcul du transfert de chaleur radiatif dans des fournaises rectangulaires en trois dimensions. Cette méthode simplifie le rayonnement en le représentant sous la forme d'une interaction en chaîne d'une zone à l'autre contrairement à une interaction directe de toutes les zones telle que préconisée par la méthode classique de zones. On a réalisé certains tests pour la validation de la méthode en faisant appel à des gaz gris et réels ainsi qu'à différentes géométries. Les résultats obtenus supportent bien la comparaison avec ceux de la méthode de zones. De plus, les temps de calcul se sont révélés considérablement réduits par rapport à ceux de la méthode de zones (facteur de réduction atteignant 24). Cette dernière caractéristique permettra à la méthode des plans imaginaires d'être plus facilement incorporée dans une simulation globale impliquant également les équations du mouvement, de la cinétique de combustion et du transfert de masse et de chaleur.

ANWENDUNG DER METHODE DER IMAGINÄREN EBENEN AUF DREIDIMENSIONALE SYSTEME

Zusammenfassung—Es wird eine dreidimensionale mathematische Formulierung der Methode der imaginären Ebenen (IPM) zur Berechnung des Strahlungsaustausches in rechteckigen Öfen vorgestellt. Bei dieser Methode wird der Strahlungswärmeaustausch als Kettenreaktion von Zone zu Zone modelliert, wohingegen beim klassischen Zonenverfahren eine direkte Wechselwirkung angenommen wird. Es wird eine Reihe von Versuchen mit grauen und realen Gasen sowie für unterschiedliche Hohlraumgeometrien durchgeführt. Die Ergebnisse stimmen gut mit denen des Zonenverfahrens überein. Das neue Verfahren erlaubt eine beträchtliche Verringerung der Rechenzeit (bis zum Faktor 24) im Vergleich zum Zonenverfahren. Dies wird dem IPM-Verfahren leichten Eingang in Gesamtsimulationen verschaffen, bei denen die Bewegungsgleichungen, die Verbrennungskinetik und der Wärme- und Stofftransport zu berücksichtigen sind.

ПРИМЕНЕНИЕ МЕТОДА МНИМЫХ ПЛОСКОСТЕЙ К ТРЕХМЕРНЫМ СИСТЕМАМ

Аннотация—Приводится трехмерная математическая формулировка метода мнимых плоскостей (IPM) для расчета радиационного переноса в проямоугольных топках. В данном методе радиационный перенос моделируется цепным взаимодействием от зоны к зоне в отличие от прямого взаимодействия в классическом зональном методе. Выполнен ряд экспериментов для серого и реального газов, а также для различных геометрий полости. Получено хорошее согласие с результатами зонального метода. Более того, значительно (в 24 раза) сокращено машинное сремя по сравнению с зональным методом. Это позволит более легко использовать метод IPM в общем моделировании, включающем уравнения движения, кинетики сторания, а также тепло- и массопереноса.